Effects of C:Mn ratios on sorption and oxidative degradation of small organic molecules on Mn-oxides

by

Hui Li[1,2]*, Benjamin Reinhart[3], Spencer Moller[4], Elizabeth Herndon[2]*

[1] *Department of Crop and Soil Sciences, North Carolina State University, Raleigh, NC 27695*

[2] *Environmental Sciences Division, Oak Ridge National Laboratory, Oak Ridge, TN 37831*

[3]*X-ray Science Division, Argonne National Laboratory, Lemont, IL 60439*

[4]*Department of Plant and Soil Sciences, University of Delaware, Newark, DE 19716*

* Corresponding author:

Hui Li; Email: hli73@ncsu.edu

Elizabeth Herndon; Email: herndonem@ornl.gov

Submitted to

Environmental Science & Technology

2022

25 **TOC Art**

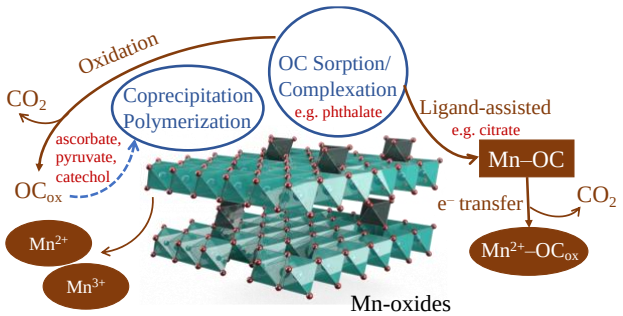
Oxidation
CO2
Coprecipitation
Polymerization
OC Sorption/
Complexation
e.g. phthalate
Ligand-assisted
e.g. citrate
Mn–OC
ascorbate,
pyruvate,
catechol
OCox
e⁻ transfer
CO2
Mn2+
Mn3+
Mn2+–OCox
Mn-oxides

26

ABSTRACT:

Manganese (Mn) oxides have high surface area and redox potential that facilitate sorption and/or oxidation of organic carbon (OC), but their role in regulating soil C storage is relatively unexplored. Small OC compounds with distinct structures were reacted with Mn(III/IV)-oxides to investigate effects of OC:Mn molar ratios on Mn–OC interaction mechanisms. Dissolved and solid-phase OC and Mn were measured to quantify OC sorption to and/or redox reaction with Mn-oxides. Mineral transformation was evaluated using x-ray diffraction and x-ray absorption spectroscopy. Higher OC:Mn ratios resulted in higher sorption and/or redox transformation; however, interaction mechanisms differed at low or high OC:Mn ratios for some OC. Citrate, pyruvate, ascorbate, and catechol induced Mn-oxide dissolution. The average oxidation state of Mn in the solid phase did not change during reaction with citrate, suggesting ligand-promoted mineral dissolution, but decreased significantly during reactions with the other compounds, suggesting reductive dissolution mechanisms. Phthalate primarily sorbed on Mn-oxides with no detectable formation of redox products. Mn–OC interactions led to primarily C loss through OC oxidation into inorganic C, except phthalate, which was predominantly immobilized in the solid phase. Together, these results provided detailed fundamental insights into reactions happening at organo-mineral interfaces in soils.

KEYWORDS: Mn–OC interaction mechanisms, OC immobilization, OC oxidation, phase transformation, OC:Mn molar ratio

SYNOPSIS:

Research findings of this study provide evidence of multiple roles of Mn-oxide minerals in stabilizing and/or destabilizing carbon in soils and sediments.

INTRODUCTION

Soil is the largest terrestrial organic carbon (OC) reservoir.[1] Much of this OC is intimately associated with soil minerals.[2] Therefore, a fundamental understanding of soil OC reactivity at mineral-water interfaces is essential to anticipating soil C storage and fluxes and their contributions to global climate change. Most past studies have largely focused on C stabilization by common Fe- and Al-(hydr)oxides (oxides hereafter);[2-4] whereas, the importance of Mn-oxides, which have much lower natural abundance than Fe- and Al-oxides, in controlling fate and transport of soil OC has been scarcely documented. Mn-oxides have high adsorption capacities and oxidizing capabilities for inorganic [5, 6] and organic compounds[7-9], and may play a significant role in regulating C presence and cycling in soils via chemical binding, physical entrapping and/or oxidizing OC.[10, 11] A study that mapped the distribution of Mn, Fe and C in soil ferromanganese nodules revealed a great OC association in the transition zones between Fe and Mn minerals but not with pure Fe minerals.[12] In another study, C was physically entrapped in nanocrystalline Mn-oxides during vermiculite weathering in an acidic forest soil.[11] In addition, though Mn participates widely in reactions with C, the mechanisms by which Mn promotes or inhibits soil C storage remains unclear. Improved understanding of Mn–OC interaction mechanisms is important for investigations into the influence of Mn on C cycling in terrestrial environments as well as for understanding contaminant removal and nutrient cycling in soils, sediments, and wastewater treatment systems.

Organic matter interacts with common soil mineral surfaces through various types of mechanisms, including electrostatic interaction, ligand exchange, surface complexation, cation bridging, Van der Waals forces, hydrogen bonding, and hydrophobic interactions.[10, 13] Adsorption and surface complexation are the prerequisite steps for reactions at mineral surfaces.[14] Surface properties affect the complexation mechanisms of OC compounds. For instance, catechol binds to Fe_2O_3, TiO_2, and Cr_2O_3 as inner-sphere complex but predominately as an outer-sphere complex to MnO_2 within the pH range between 3 and 10.[15] In addition, due to distinct characteristics of different moieties, various organic compounds may possess diverse adsorption capacities onto minerals.[10, 16] Thus, the rate and mechanisms of interactions between OC compounds and Mn-oxide minerals are highly dependent on adsorptive and complexing properties of OC and minerals.

Once surface complexes are formed, some OC compounds are capable of transferring electrons to Mn, initiating ligand-assisted and/or reductive mineral dissolution coupled to oxidative decomposition of these organic compounds.[14, 16-18] For instance, oxalic acid, phosphonoformic acid and citric acid, acting as both reducing agents and chelating agents, strongly adsorb on Mn-oxides and drive mineral reduction and dissolution.[14, 17] Although the potential for Mn-oxides to sorb and/or oxidize organic matter has been established,[10] their

specific interaction mechanisms and the extent to which these interaction reactions occur with diverse organic compounds that comprise various structures remain poorly constrained.

Soil organic matter is a complex mixture of a wide variety of organic compounds, differing in molecular size, polarity, composition and position of various functional groups that greatly influence the affinity and reactivity of OC to Mn-oxides.[10, 19] Interaction mechanisms between individual OC compounds and Mn-oxides may be different and depend on environmental conditions or relative abundances.[16, 20] For example, citrate formed more inner-sphere complexes with hematite at lower C:Fe ratios.[21] Higher initial OC:metal molar ratios resulted in a higher adsorption rate of dissolved organic matter on hydrous manganese oxide and goethite.[8, 20] Citrate had stronger reducing capability on Mn-oxides than oxalate due to their differences in characteristics and binding sites on minerals.[16] Fulvic acid induced different transformation products of Mn-oxide at different OC:Mn ratios.[20] Furthermore, few studies adequately evaluate both sorption and degradation processes that occur during reactions between organic compounds and Mn oxides. Experiments that measure either loss of C from solution or C accumulation in the solid-phase fail to account for loss of inorganic C produced during reactions. Studies that quantify dissolved Mn as a metric for determining reaction rates may overlook reduced Mn in the solid-phase or Mn that has re-oxidized on the mineral surface.

In this study, we investigated the ability of Mn-oxides to either immobilize or oxidize various forms of soil OC compounds in order to evaluate the impact of Mn-oxides on carbon storage in soils. Accordingly, the primary aim of the present study was to investigate the interaction mechanisms of representative OC compounds with Mn-oxides. In a controlled system, adsorption reactions of five OC compounds (phthalate, catechol, ascorbate, pyruvate, and citrate) on Mn-oxide minerals at a broad range of OC:Mn molar ratios were studied. These low molecular weight organic compounds of known structures share common functional groups (e.g., hydroxyl, carboxyl, and benzene ring) with heterogeneous natural organic matter whose fundamental interaction mechanisms with soil minerals are challenging to identify. Studies in this simplified system containing single phase organic compounds, instead of a mixture of a wide variety of extracted natural OM, and pure mineral assemblages are useful from a methodological point of view to obtain fundamental information about solute-surface interaction mechanisms and without biotic interferences. In addition, we quantified the relative proportions of OC removed from solution due to either association with minerals or production of inorganic C in order to compare contributions of Mn-oxides in C stabilization versus C loss.

MATERIALS AND METHODS

Sorption Reactions

Five common and naturally existing aromatic or nonaromatic OC compounds (characteristics listed in Table S1)—phthalate, catechol, ascorbate, pyruvate, and citrate—were studied for their distinct sorption mechanisms on Mn-oxide minerals. These experiments were conducted with three synthetic Mn-oxides: birnessite, hydrous Mn oxide, and cryptomelane (methods in SI). Given that the differences between different minerals (Table S2 and Figure S1) were much smaller than that among OC compounds, we averaged the results of phase transformation of OC and Mn induced by each OC compound over all three Mn-oxides to focus the comparison among OC compounds.

Batch adsorption reactions of each OC compound with Mn-oxides were conducted in 50 mL falcon tubes for 24 h at room temperature (22 ± 1 °C). All glass vials and milli-Q water used in the experiments were autoclaved. A fixed amount of Mn-oxide suspension (8 mmol L^{-1}) was pre-equilibrated in 0.01 mol L^{-1} of NaH_2PO_4/Na_2HPO_4 buffer at pH 7.0 ± 0.1. Concentration level of phosphate buffer is higher than in some natural soils,[22] however, is necessary to achieve high pH buffering capacity. Stock solutions of 2.5 mol C L^{-1} of individual OC were maintained at pH 7.0 ± 0.1 by adding 1 mol L^{-1} HCl or NaOH. The adsorption reaction was initiated by adding different volumes of OC stock solutions to mineral suspensions to reach a total volume of 30 mL and to obtain different OC:Mn molar ratios, ranging from 0 to 41:1. All reactors were shaken at 190 rpm continuously for 24 h. Suspensions were then centrifuged and filtered through 0.1 μm polyethersulfone membranes (Millipore Sigma), and supernatant and solid phases were kept separately for further analysis. A control set without OC addition was included to test the dissolution rate of synthetic Mn-oxides in the buffer solution. Another control set without Mn-oxides was also conducted in parallel to determine the stability of these OCs under experimental conditions. No additional electrolyte solutions were introduced in this study since the concentration of pH buffers were high enough to maintain constant ionic strength.

Quantification of Dissolved Organic Carbon and Dissolved Manganese Contents

Concentration of dissolved organic carbon (DOC) in supernatant was quantified on a total organic carbon analyzer (TOC-L, Shimadzu corporation, Kyoto, Japan) using the 680 °C combustion catalytic oxidation method, with a detection limit of 4 μg C L^{-1}. Samples were diluted with 0.1% concentrated HCl solution prior to analysis to remove inorganic carbon. Decreases in DOC in solution over time were attributed to sorption to the solid phase and/or reactions that produced inorganic C. Concentration of dissolved Mn in supernatant was determined on an inductively coupled plasma optical emission spectrometry (ICP-OES, Thermo Scientific iCAP 7000 Series). Subsamples for this analysis were diluted with 1% concentrated

HNO_3 solution right after sample collection from the sorption experiments. Transformation of organic compounds after interacting with Mn-oxides was determined using solution ^1H nuclear magnetic resonance (NMR) spectroscopy (details in SI), where appearance of new peaks at chemical shifts different from original OC compounds indicated the formation of oxidation products.

Solid Phase Characterization

The weight percentage of total C in solid phases was quantified on an Elementar Unicube® trace organic elemental analyzer. A soil containing 2.69 wt.% of C was used as a reference to calibrate the internal standard curve. Carbon contents in solid samples were determined by high temperature combustion according to the Dumas method via a thermal conductivity detector, with a low detection limit of 10 μg/g.

Phase identification of Mn-oxides before and after OC interactions under specific OC:Mn molar ratios was characterized by X-ray diffraction (XRD) using a Panalytical Empyrean diffractometer with Cu_{Ka} radiation at 45 kV and 40 mA over a 2θ range from 5° to 90° with a step size of 0.033° and a Bruker D8 x-ray diffractometer with Cu_{Ka} radiation at 45 kV and 40 mA over a 2θ range from 5° to 90° with a step size of 0.05°.

X-ray Absorption Spectroscopy

X-ray absorption spectroscopy (XAS) was conducted at beamline 12-BM at the Advanced Photon Source (APS) in April 2021. Freeze dried solid samples were mixed well, packed into Teflon sample holders, and sealed with Kapton tape. XAS spectra were collected from –200 eV to +642 eV around the Mn K-edge (6539 eV) in transmission mode with a 500 μm wide beam at 1×10^{11} @ 12 keV photons per second. Data processing, including energy calibration, merging of duplicate scans and linear combination fits, was performed in Athena (version 0.9.26).[23] All spectra were referenced to a Mn foil with an E^0 = 6539 eV.

Linear combination fits to determine the average oxidation state (AOS) of Mn were performed in the X-ray absorption near edge structure (XANES) region from –20 to +30 eV using reference spectra for single valence compounds (Mn(II)-oxalate, Mn(II)-oxide, rhodochrosite, Mn_2O_3, Mn(III)-oxyhydroxide, ramsdellite, Li_2MnO_3 and pyrolusite) following the Combo method [23, 24]. Best fits were selected as those reporting minimal reduced chi-square values. Relative fractions of Mn(II), Mn(III) and Mn(IV) were calculated from the best fits to determine the average oxidation states of bulk Mn (Table S3). Furthermore, to compare the structural changes of Mn-oxides, Mn K-edge extended X-ray absorption fine structure (EXAFS) spectra were converted to the k^3-weighted function and Fourier transforms were calculated over an R range of 1–6 Å.

Statistical Analysis

Significant differences in the changes of Mn AOS after interacting with organic compounds were assessed with one-way ANOVA, Tukey's honestly significant difference (HSD) test approach at 95% confidence level, using the agricolae package in R (version 2021.09.1).

RESULTS AND DISCUSSION

Immobilization and oxidative decomposition of organic compounds by Mn-oxides

Decreases in DOC in solution are attributed to sorption and precipitation that immobilize C in the solid phase and/or redox reactions that produce inorganic C, presumably through oxidation to CO_2 (Figure S2a). The amount of generated inorganic C is calculated from the difference between the total organic C loss from aqueous solutions and the amount of immobilized C in solids. For all OC compounds, higher initial OC:Mn molar ratios result in linear increases in C accumulation in solids (Figure 1a). Carbon immobilization may result from processes such as adsorption, surface precipitation, co-precipitation with reduced Mn, and polymerization of decomposed OC fractions.[10] Ascorbate and its decomposition products have higher accumulation in the solid-phase than the other OC compounds. For most of the studied organic compounds, OC contributed approximately 10% of the total weight of the solid phases at OC:Mn>5, indicating strong C stabilizing capability of Mn-oxides and their transformation products (Figure S2c). However, citrate-C does not accumulate in the solid-phase at OC:Mn > 20 due to a complete dissolution of Mn-oxides and absence of solid-phase transformation products.

Higher OC:Mn ratios also result in more C being oxidatively decomposed (Figure 1b). Citrate has the highest tendency to be oxidized by Mn-oxides to produce inorganic C, followed by ascorbate, pyruvate, and catechol, which generally follows the increasing trend of pKa values of their conjugate acids (Table S1). Production of inorganic C stabilizes or decreases at high OC:Mn, which may indicate depletion of necessary reactants to drive oxidation, e.g., complete Mn-oxide dissolution or decrease in oxidizing capacity of Mn minerals.

As the initial concentrations of OC compounds increase, a lower percentage of initial C is removed from solution due to accumulation in the solid-phase and/or loss as inorganic C (Figure S2b). For example, ≥10% of citrate-C is reacted at OC:Mn <5 while ~5–10% is reacted at OC:Mn>5. The percentage of reacted citrate-C is similar to pyruvate and higher than ascorbate, catechol and phthalate. However, low percentage of C loss from solution is not necessarily equal to low interaction extent. Some organic compounds may react with Mn-oxides, and then either the original OC compounds or their decomposition products will be released back to the solution. Given the high concentration of original OC ranging from 5 to 333 mmol L^{-1} and low percentage of reacted C, which means abundant unreacted OC, in most reaction systems, competition of phosphate and dissolved organic/inorganic C for adsorption on Mn-oxide surface sites will be minimal. However, at low OC:Mn ratios, which means similar concentration levels of initial OC and phosphate buffer, phosphate competition with OC for mineral surface sites may have slightly reduced OC and mineral interaction extent.

The relative contributions of C immobilization in solids and oxidative generation of inorganic C to the total C loss differ amongst OC compounds (Figure 1c and 1d). Citrate-C removed from solution is almost completely oxidized to inorganic C. Carbon losses for pyruvate, catechol and ascorbate are also dominated by oxidative decomposition to inorganic C, while phthalate-C is fixed in solids. For ascorbate, pyruvate, and catechol, the relative proportion of C immobilized in the solid-phase decreases up to OC:Mn ~5 and then increases at OC:Mn >5, contributing more than 60% of the total C loss for ascorbate at OC:Mn>30. These patterns suggest that C immobilization reactions differ at low and high OC:Mn ratios. Sorption reactions alone are certainly not sufficient to describe the complete interaction phenomenon. Thus, other analyses are used in order to provide more detailed descriptions to the molecular mechanisms.

Dissolution and reduction of Mn-oxides

The higher OC:Mn molar ratios also result in a greater Mn-oxide dissolution by several OC compounds (Figure 2 and S3). Citrate, pyruvate, ascorbate, and catechol dissolve appreciable amounts of Mn-oxides and/or lead to a mineral phase transformation. Citrate induces more than three-times more Mn dissolution than other organic compounds (open circle in Figure 2), reaching approximately 100% of initial Mn in Mn-oxides, followed by pyruvate, ascorbate and catechol. However, there is no detectable amount of dissolved Mn in the solution of phthalate, due to either no mineral reduction and dissolution or rapid re-adsorption of reduced Mn by Mn-oxides.

Calculated from the fitting results of XANES spectra (Table S3 and Figure S4), Mn AOS in solid phase significantly decreases from ~4 to ~2 or remains unchanged following reactions with different OC compounds at various OC:Mn ratios (Figure S5). The amount of total reduced Mn in Figure 2 (open square) is the sum of dissolved Mn in aqueous phase and reduced Mn in solid phase (Table S3). The amount of Mn reduction induced by citrate remains very close to that of Mn dissolution, indicating that all reduced Mn is released into solution. Reactions between Mn-oxides and pyruvate, ascorbate, and catechol release relatively little dissolved Mn but result in nearly 100% reduced Mn(II) in the solid-phase, even at lower OC:Mn molar ratios than citrate. Thus, initial Mn-oxides were reduced, but Mn(II) was immobilized in the solid phase rather than released into solution. The phosphate buffer used in this study may inhibit mineral dissolution, to some extent, due to coprecipitation with Mn(II) and/or ligand competition [25]. Our analysis below also suggests that low Mn dissolution in catechol, ascorbate and pyruvate involved reactions may be ascribed to the coprecipitation of phosphate with reduced Mn to form Mn(II)-phosphate.

Change of equilibrium pH due to Mn–OC interactions

Although a pH buffer is introduced to maintain the pH around 7, the equilibrium pH values in solution still change following OC and Mn-oxides interactions (Figure 3). No pH change was observed in controls containing no OC and/or no mineral. In general, the studied OC compounds

induce three different trends of pH changes—increase, no change and decrease. These findings suggest that at least three interaction mechanisms are taking place between different OC compounds and Mn-oxides.

At OC:Mn<10, the equilibrium pH after interacting with citrate increases up to about 1.5 units; but at higher OC:Mn ratios, this pH increase is much subtler. Similarly, at OC:Mn<1, the addition of catechol also prompts salient pH increase, with the peak pH increase up to 1.5 units at OC:Mn~0.5. However, higher C loading results in much smaller pH increase. These findings suggest that two distinct interaction mechanisms may be at play at low and high OC:Mn ratios. The addition of phthalate does not incur significant pH changes. On the contrary, interactions with pyruvate and ascorbate induce a slight pH decrease of mineral suspensions at a broad range of OC:Mn ratios.

Given the low point of zero charge values of these Mn-oxides, they are net negatively charged at the experimental neutral pH conditions, containing –MnOH and $–MnO^-$ as dominant surface sites. Thus, when complexing with organic compounds, the following model reactions may take place [26]:

$$–MnOH + RCOO^- = –MnOOCR + OH^-$$

$$–MnO^- + RCOO^- + H_2O = –MnOOCR + 2OH^-$$

where $RCOO^-$ represents a dissociated carboxylate group. These reactions result in the release of hydroxyl groups via ligand exchange. In addition, this pH increase may also result from the oxidation of organic compounds (e.g. catechol) that release hydroxyl groups.[17, 25] Moreover, the dissolution process of MnO_2 consumes 4 times equimolar of H^+ of Mn [27] that can dramatically derive the pH increase, e.g. for citrate. On the contrary, pH decrease may be ascribed to the generation of CO_2 as a product of oxidative degradation of OC compounds that dissolves in the suspension.[17, 28] Furthermore, the adsorption of reduced Mn^{2+} back onto the mineral surface may result in a release of approximately 2 moles of H^+ per mole of sorbed Mn.[29] An unchanged pH of Mn-oxide suspensions after interacting with phthalate may suggest a physical sorption process, without net exchange of H^+ or OH^- groups.

Therefore, when interacting with citrate and catechol, the relative dominancy of –OH release during ligand exchange and mineral dissolution and the oxidative generation of CO_2 and re-adsorption of dissolved Mn^{2+} are regulating the extent of pH change of mineral suspensions at different OC:Mn ratios. At lower OC:Mn ratios, reactions that release –OH dominate and lead to a dramatic pH increase; however, at higher ratios, the contribution of the CO_2 generation becomes more prevailing that offsets a fraction of the released –OH. A slight pH drop in ascorbate and pyruvate systems may ascribe to relative abundant formation of inorganic C and

adsorption/precipitation of dissolved Mn^{2+}, which, however does not occur in citrate system. No pH change in phthalate system suggests other sorption mechanisms rather than ligand exchange.

Mn K-edge extended X-ray absorption fine structure spectroscopy

The Fourier transformed EXAFS spectrum of birnessite in R space shows two peaks at ~1.5 and ~2.5 Å (R+ΔR) that correspond to the Mn–O in MnO_6 octahedra and the edge-sharing Mn–Mn, respectively, and a weak peak at ~3 Å (R+ΔR) corresponds to scatterings of adsorbed Mn(II) and/or Mn(III) at MnO_6 octahedra layer vacancies (Figure 4), which is in agreement with other synthetic birnessite minerals.[30, 31] After the interaction with phthalate, these peaks remain mostly unchanged at a wide range of OC:Mn molar ratios from 0.2 to 15 (Figure S6). Interaction with citrate induces a slight decrease in intensities of these peaks, which may be due to a decrease in particle size[30] and mineral dissolution. Interaction with catechol, pyruvate and ascorbate leads to apparent shifts of these peaks. However, catechol induces dramatic shifts of these peaks at both low and high OC:Mn molar ratios, which indicate either an increase in Mn–O and Mn–Mn shell distances or a complete phase transformation of birnessite (Figure S6). Changes in peak positions are consistent with dramatic and almost complete Mn reduction induced by catechol at OC:Mn>0.5. However, the interaction with ascorbate at OC:Mn=0.2 and with pyruvate at <4 induces only a slight decrease in intensities of these peaks, but dramatic shifts at higher OC loading ratios, suggesting complete mineral phase transformation only at high OC:Mn molar ratios (Figure S6).

Mn phase transformation identified by XRD

XRD is applied to further evaluate the solid phases that change in their appearance (Figure S7) and in EXAFS spectra following reactions with several organic compounds (e.g. ascorbate, catechol and pyruvate) at high OC:Mn molar ratios. Compared with original Mn-oxide, the association of phthalate and citrate results in an addition of characteristic peaks of these organic compounds in the XRD patterns (Figure 5 and S8), suggesting that these OC compounds form complexes with Mn-oxide but no Mn phase changes occur. Following reaction with ascorbate and catechol, peaks of the initial Mn-oxide disappear and new peaks consistent with Mn(II)-phosphate [$Mn_3(PO_4)_2$] appear. The solid-phase that remains following reaction with pyruvate has low crystallinity but shows slight peaks at 27°, 30°, and 35°, which are major characteristic peaks of Mn(II)-phosphate.

Influences of phosphate buffer on the fate of reduced Mn

The phosphate that is used in the pH buffer coprecipitates with dissolved Mn following reduction of Mn-oxides by certain organic compounds. As a strong inorganic ligand, phosphate has a higher Mn(II)-complex constant than all the studied organic compounds, except citrate (Table S1), suggesting strong complexing capability of phosphate with reduced Mn. These

results are in accordance with the visible change of the mineral phases from brown to white for pyruvate and ascorbate (Figure S7). Persistence of brown color in the catechol precipitates may indicate formation of polymerized organic compounds, as has been observed for hydroquinone[32], in addition to Mn(II)-phosphate. Given the fact that Mn(II)-phosphate forms after Mn-oxides react with ascorbate, catechol and pyruvate, the high ratio of C immobilization in the solid phases may be ascribed to co-precipitation and/or polymerization rather than sorption to the Mn-oxide surface.

In natural soil environments, dissolved Mn^{2+} that is released into solution through mineral dissolution may be leached out of the system, taken up by plants or microorganisms, or complexed by strong ligands, such as citrate and phosphate (Table S1). Specifically in this study, Mn^{2+} cations precipitate with phosphate to form Mn(II)-phosphate that limits the apparent dissolution of Mn oxides (Figure 2)and keeps dissolved Mn^{2+} from building up in the system. In the present study, precipitation of Mn^{2+} with HPO_4^{2-} or $H_2PO_4^-$ releases H^+ that leads to a slight pH decrease of some reaction systems, for example pyruvate and catechol (Figure 3).

Primary Mn–OC interaction mechanisms

All organic compounds that generate reduced Mn in the solid-phase also have strong mineral dissolution capability; whereas the ones that do not affect the Mn AOS in the solid phases include citrate, which dissolves appreciable amounts of Mn-oxides, and phthalate which induces no Mn dissolution. Thus, combining all the above analysis, we propose the occurrence of three fundamental types of interacting mechanisms between studied organic compounds and Mn-oxides. For all these reactions, complex formation between organic compounds and Mn-oxide surface sites is pre-requisite.

i) Sorption: phthalate

There is an appreciable amount of immobilized phthalate-C in solid minerals and no observable OC oxidation into inorganic forms due to phthalate addition. The chemical shifts of ^{1}H NMR peaks of phthalate remain without appearance of new peaks for other products (Figure S9). Besides, there is no detectable Mn dissolution and the AOS of Mn in solids remains statistically unchanged from the original synthetic minerals (Figure 2 and S5), suggesting negligible Mn reduction. Thus, phthalate may interact with Mn-oxides solely through sorption, including adsorption and/or surface precipitation as the C loading increases, rather than redox reactions. No redox reaction was observed between phthalate and Mn-oxides at pH 7.2.[33] Adsorption of phthalate was also observed in other studies on adsorption of di-n-butyl phthalate, which is a derivative of phthalate, by Mn-oxide and biochar majorly via H-bonding [34] and on adsorption of phthalic acid and diethyl phthalate by zeolitic imidazolate framework via electrostatic interaction.[35] Studied organic compounds comprised of carboxyl and hydroxyl groups have high reactivity with Mn-oxides, except phthalate, which may ascribe to its strong

366 structural stability that inhibits electron transfer from C and a pKa close to experimental pH
367 condition, and its relatively lower water solubility than the other organic compounds (Table S1).

368 ii) Ligand promoted mineral dissolution followed by intramolecular electron transfer and
369 strong ligand complexation with dissolved Mn^{2+}: Citrate

370 Citrate is a strong ligand that induces Mn-oxide dissolution to release dissolved Mn
371 (presumed to be Mn^{2+}). The Mn AOS in synthetic Mn-oxides does not significantly decrease
372 during dissolution, suggesting that the reaction is initiated by citrate ligand complexation and
373 then followed by Mn reduction in solution. EXAFS and XRD results also show no dramatic
374 structural transformation of Mn-oxides during the reaction. Similarly, when reacting with
375 feitknechtite (β-MnOOH), citrate initiates the mineral dissolution through ligand-promoted
376 dissolution by forming Mn(III)-citrate complexes, which are then reduced to dissolved Mn^{2+}.[36]
377 Citrate is a strong ligand that complexes with dissolved Mn^{2+} in aqueous solutions. At similar
378 neutral pH and ionic strength conditions as present in this study, up to 85% of 10 μM Mn^{2+} is
379 complexed by citrate.[17] According to the stability constants of Mn(II)-complexes, citrate has a
380 much larger constant than phosphate, phthalate, pyruvate, ascorbate or catechol (Table S1),
381 enabling much stronger complexing capability of citrate than the other organic and inorganic
382 ligands. Therefore, we expect that reduced Mn^{2+} cations remain in solution via complexation
383 with citrate, leaving negligible reduced Mn in the solid phase.

384 The adsorption of citrate via ligand exchange and the rapid dissolution of Mn-oxides both
385 release hydroxyl groups that may explain the dramatic pH increase at OC:Mn<10. In addition, a
386 fraction of the phosphate buffer may adsorb on Mn-oxides,[37] which not only releases hydroxyl
387 groups during ligand exchange but also destabilizes the pH buffer. As Mn-oxides dissolve, more
388 phosphate is released to enhance buffering capacity, especially after complete dissolution of Mn
389 at OC:Mn>20.

390 Oxidative decarboxylation of citrate yields 3-ketoglutarate, as follows, that can be further
391 transform to acetoacetate through non-redox or metal catalyzed decarboxylation, and each of
392 these steps generates one mole of CO_2 per mole of reactant.[17] Peaks at chemical shifts in
393 accordance to acetoacetate are present in the ^1H NMR spectra of liquid samples at citrate-
394 C:Mn=0.2 (Figure S9). Thus, though more Mn-oxides dissolve at higher OC:Mn ratios,
395 increasing amount of generated CO_2 can offset partially, the extent of pH increase.

396 $$\text{Citrate} + MnO_2 + 4H^+ = \text{3-ketoglutarate} + Mn^{2+} + CO_2 + 2H_2O \quad (1)$$

397 iii) Reductive mineral dissolution: pyruvate, ascorbate, and catechol

398 Like citrate, pyruvate, ascorbate, and catechol induce Mn-oxide dissolution. However,
399 different from citrate, AOS of Mn decreases to ~3 following reactions at low OC:Mn ratios and
400 to ~2 at higher OC:Mn ratios (Table S3). These results suggest the reductive dissolution of Mn-

oxides. In the absence of a strong ligand such as citrate (Table S1), the reduced Mn^{2+} is not complexed by these organic compounds.

Oxidative decarboxylation of pyruvate by Mn-oxides produces acetate,[14] as follows:

CH_3COCOO^- (pyruvate) + MnO_2 + $2H^+$ = CH_3COO^- (acetate) + CO_2 + Mn^{2+} + H_2O (3)

from which, the generated acetate can further be oxidized by MnO_2 to two molecules of CO_2.[38] The amount of sorbed/reacted pyruvate-C is lower than that of ascorbate-C (Figure S2a). However, given their differences in number of C in molecular formula, more moles of pyruvate are reacted than ascorbate (Figure S2b).

Oxidation of ascorbate generates dehydroascorbate, as follows, which can further be hydrolyzed to form 2,3-diketoglulonic acid.[39] Oxalate may also form, for example during oxidative decomposition of Cu(I)-complexed ascorbate or dehydroascorbate by O_2.[40] Each oxalate can be oxidized to two CO_2.[14]

Ascorbate + MnO_2 + $4H^+$ = dehydroascorbate + Mn^{2+} + $2H_2O$ (2)

Once ascorbate forms complexes with Mn-oxide, a one-electron exchange step take place between the binding site C and Mn, which is reduced to Mn(III) as an intermediate product that is further reduced to Mn^{2+}.[41] In addition, ascorbate can be auto-oxidized by oxygen, catalyzed by transition metal ions (e.g. Fe^{3+} and Cu^{2+}). In this process, metal, ascorbate and oxygen form a complex, where the metal ion serves as a bridge for electron transfer from ascorbate to oxygen.[39] Similarly, dissolved Mn^{2+} may also facilitate this oxidation process of ascorbate. Production of inorganic C decreases at OC:Mn>15 (Figure 1), indicating that less ascorbate can be completely oxidized to generate CO_2 due to depletion of available oxidants (i.e., Mn-oxide). Much ascorbate derived C remains in the solid phase (Figure 1), indicate that some of its decomposition products sorb without further reacting and/or that the C is co-precipitated with the Mn(II)-phosphate.

Catechol oxidation by synthetic Mn-oxides at pH~7 or Mn-oxides in soils at pH~8 forms semiquinone radicals which then transform to quinone or polymerize to insoluble polymers.[42, 43] Reduced Mn produced through Mn-oxide dissolution can also form complexes with catechol, which can be further oxidized in air.[43] At pH 4, 5-16% of catechol–C is oxidized into CO_2 via abiotic ring cleavage and oxidation by Mn-oxide (birnessite), with 55-83% of C polymerized into the solid phase.[28] The first step in oxidation of catechol, as follows, consumes two moles of protons per mole of reduced Mn but does not produce CO_2. This dominance of this reaction at low OC:Mn ratios is consistent with the abrupt pH increase (Figure 3), in agreement with another similar study which also prevents Mn^{2+} release [42].

$C_6H_4(OH)_2$ + MnO_2 + $2H^+$ → $C_6H_4O_2$ + Mn^{2+} + $2H_2O$ (4)

Similar to pyruvate and ascorbate systems, the H^+ released through Mn(II)-phosphate precipitation may counteract the H^+ consumed in the first step of catechol oxidation and contribute to smaller pH increases at OC:Mn>1. However, the different color of the solid phase

in catechol system from pyruvate and ascorbate possibly suggest the formation of insoluble polymerized C that causes darkening of the color of phenol compounds (the "browning phenomenon").[44]

Competing with Mn-oxides, dissolved O_2 also acts as an electron acceptor that oxidizes these catechol derived semiquinone radicals to quinones. Another reaction mechanism has also been proposed for interactions at high OC:Mn ratios, as follows,[42] which might cause the much smaller pH increase in Figure 3 at OC:Mn>1. The competition between Mn and O_2 is dependent on the ratio of C to Mn-oxides, where high OC:Mn molar ratios induce more O_2 consumption and vice versa.[42]

$$MnO_2 + 2C_6H_4(OH)_2 = Mn^{2+} + 2C_6H_4O_2^{\bullet} + 2H_2O$$

$$O_2 + 4C_6H_4O_2^{\bullet} + 2H_2O = 4C_6H_4O_2 + 4OH^-$$

Other interaction mechanisms

Assuming all generated inorganic C was oxidized from average valence state of C in each organic compound, then the maximum oxidizing capacity of Mn-oxides, if all reduced, in the experiments was 0.16 mmol organic-C (Table S1, calculation equation in the note), which was a small fraction of generated inorganic C. However, given the fact that C in different functional groups contain different valences (e.g., +3 in -COOH), more C (~0.48 mmol) could be directly oxidized by Mn-oxides. The excess inorganic C might be derived from photochemical oxidation, with O_2 as the main oxidant. No significant C loss/transformation is detected in the mineral-free controls within the experimental period, indicating the stability of OC compounds under light without Mn-oxides. Therefore, in addition to the reductive-oxidation reactions, Mn catalyzed photochemical formation of reactive species, such as hydroxyl radicals, may also contribute to the total decomposition of organic compounds,[45] which also relies on the photochemical reactivity of organic compounds.[46, 47]

Furthermore, in addition to oxidizing OC compounds, dissolved O_2 is also capable of oxidizing reduced Mn^{2+} to generate new Mn-minerals that are electron acceptors and oxidants.[48] Regeneration of Mn-oxides would increase the oxidizing capacity of the system above that of the original Mn-oxides. Future kinetic studies are needed to differentiate these mechanisms.

According to the above XAS and XRD, there are no original Mn-oxides left following reaction with ascorbate, pyruvate, and catechol at high OC:Mn molar ratios. Thus, the C immobilization in the solid-phase is not via C adsorption or surface complexation onto Mn-oxides, but may possibly be due to coprecipitation together with reduced Mn and/or polymerization. For example, the oxidation of catechol by birnessite can produce insoluble and refractory organic precipitates via polymerization of oxidizing products that enhance more C be stabilized into the solid phase.[28]

The total number of surface sites calculated for birnessite in our study (0.0261 g), assuming a similar specific surface area (40 m^2/g) and surface site density (18.3 sites/nm^2) as birnessite synthesized using the same method, is around 19.1×10^{18}.[49] This means birnessite can accommodate at most $(19.1\times10^{18})/(6.02\times10^{20}$ molecule/mmol)=0.032 mmol OC molecules, given the assumption of monodentate complexation and coordination of molecules position. This value corresponds to 0.26 mmol C for phthalate, 0.19 mmol C for ascorbate, catechol and citrate, and 0.10 mmol C for pyruvate, if these OC compounds only adsorb on Mn-oxides. In another similar study, low fraction of mineral surface sites was occupied by phenol type of organic compounds.[50] The much higher C immobilized in solids, particularly at high OC:Mn ratios (Figure 1a), may result from other interaction mechanisms, such as surface precipitation, polymerization and co-precipitation. Though Mn(III) occurs in transformed Mn minerals at certain OC:Mn ratios according to the fitting results of XANES spectra (Table S3), more studies are needed to determine whether the Mn(III) in solid phase is formed by comproportionation of sorbed Mn(II) and structural Mn(IV) [51] or direct one-electron-transfer reduction of structural Mn(IV) to Mn(III).

Implications on Mn–OC interactions in soils

The abundance of both organic compounds and Mn minerals vary widely in natural environments.[52] Soil organic matter content in mineral topsoil generally constitutes more than 1% of soil mass and can be much higher in organic soils, and decreases in deeper soils. Even within a specific rhizosphere, the concentrations of organic compounds vary dramatically in space and time, due largely to plant root exudations and microbial activities.[53] The natural abundance of manganese in soil is low and generally varies around 0.1%.[54] However, Mn concentrations are often higher in organic-rich topsoils (e.g., ~1 wt.%)[55] and can contribute substantially to organic matter oxidation.[56] There are some unique soils that contain extremely high quantities of Mn, up to 141 g kg^{-1}.[57] Therefore, the relative molar ratios of OC:Mn may vary dramatically in the natural soil environments. Moreover, Mn-oxides can generate chemical impacts that are far out of proportion to their generally low natural abundance.[10, 12]

The relative roles that Mn plays in promoting or inhibiting OC storage in soils are quantified, showing a primary role of oxidation rather than immobilization for most C compounds. In addition to phthalate, many saturated alcohols, aldehydes, ketones, and carboxylic acids showed undetectable redox reactivity with Mn-oxides at pH 7.2.[33] Citrate, pyruvate and catechol, which are also common structures of humic substances, show high reducing capability towards Mn-oxides in this study; thus, humic substances may also have great reducing potential to Mn-oxides in soils. However, all these processes also result in C stabilization through an accumulation of either the original OC or its oxidation products in the solid mineral phases through complexation, coprecipitation, and/or polymerization reactions. Insights from our study can provide

fundamental information on possible interaction mechanisms that could happen in soils. Improved understanding of Mn–C interaction mechanisms is important for investigating contaminant removal and nutrient cycling in soils, sediments, and waste-water treatment systems. Future research will have to address the direction and the extent to which the proposed mechanisms are able to alter the stability of natural soil organic matter, which contain more complicated structures and properties, under certain environmental conditions.

ACKNOWLEDGMENTS

This work was sponsored by the Laboratory Directed Research and Development Program of Oak Ridge National Laboratory (ORNL), managed by UT-Battelle, LCC for the US Department of Energy (DOE) under contract DE-AC05-00OR22725, by the ORNL Critical Interfaces Science Focus Area sponsored by the DOE Office of Science Biological and Environmental Research Program, and by US Department of Agriculture–National Institute of Food and Agriculture (USDA-NIFA), Hatch project NC02898. The authors would like to acknowledge Xiangping Yin, Jana Phillips, and Geoff Schwaner (ORNL) for assistance with dissolved OC and total solid C content analysis and Xiaoyan Sun (NC State University) for assistance with NMR analysis. This research used resources at Beamline 12-BM of the Advanced Photon Source, a user facility operated for the US DOE Office of Science by Argonne National Laboratory under contract DE-AC02-06CH11357. This work was performed in part by the Molecular Education, Technology and Research Innovation Center (METRIC) at NC State University, which is supported by the State of North Carolina.

ASSOCIATED CONTENT

Supporting Information

The Supporting Information is available free of charge at

Mn-oxides synthesis methods; parameters for ^{1}H NMR analysis; characteristics of organic compounds (Table S1) and Mn-oxides (Table S2), fitting results from XANES spectra (Table S3), XANES whole spectra of Mn-oxide minerals (Table S4), XAS spectra of unreacted Mn-oxides (Figure S1), OC distribution (Figure S2), Mn dissolution (Figure S3), XANES spectra of solid phases (Figure S4), Mn AOS (Figure S5), EXAFS spectra of the Mn-oxides (Figure S6), images of Mn-oxides after reactions (Figure S7), XRD pattern of solid phases after reaction (Figure S8) and ^{1}H NMR spectra of solution (Figure S9).

REFERENCES

1. Lehmann, J.; Kleber, M., The contentious nature of soil organic matter. *Nature* **2015,** *528*, 60-68.
2. Kleber, M.; Eusterhues, K.; Keiluweit, M.; Mikutta, C.; Mikutta, R.; Nico, P. S., Mineral-organic associations: Formation, properties, and relevance in soil environments. *Adv. Agron.* **2015,** *130*, 1-140.
3. Keiluweit, M.; Bougoure, J. J.; Nico, P. S.; Pett-Ridge, J.; Weber, P. K.; Kleber, M., Mineral protection of soil carbon counteracted by root exudates. *Nat. Clim. Chang.* **2015,** *5*, 588-595.
4. Li, H.; Bölscher, T.; Winnick, M.; Tfaily, M. M.; Cardon, Z. G.; Keiluweit, M., Simple plant and microbial exudates destabilize mineral-associated organic matter via multiple pathways. *Environ. Sci. Technol.* **2021,** *55*, 3389-3398.
5. Feng, X. H.; Zhai, L. M.; Tan, W. F.; Liu, F.; He, J. Z., Adsorption and redox reactions of heavy metals on synthesized Mn oxide minerals. *Environ. Pollut.* **2007,** *147*, 366-373.
6. Li, H.; Liu, F.; Zhu, M.; Feng, X.; Zhang, J.; Yin, H., Structure and properties of Co-doped cryptomelane and its enhanced removal of Pb^{2+} and Cr^{3+} from wastewater. *J. Environ. Sci.* **2015,** *34*, 77-85.
7. Estes, E. R.; Andeer, P. F.; Nordlund, D.; Wankel, S. D.; Hansel, C. M., Biogenic manganese oxides as reservoirs of organic carbon and proteins in terrestrial and marine environments. *Geobiology* **2017,** *15*, 158-172.
8. Stuckey, J. W.; Goodwin, C.; Wang, J.; Kaplan, L. A.; Vidal-Esquivel, P.; Beebe Jr., T. P.; Sparks, D. L., Impacts of hydrous manganese oxide on the retention and lability of dissolved organic matter. *Geochem. Trans.* **2018,** *19*, 6.
9. Xia, X.; Stone, A. T., Mandelic acid and phenyllactic acid "Reaction Sets" for exploring the kinetics and mechanism of oxidations by hydrous manganese oxide (HMO). *Environ. Sci. Process. Impacts* **2019,** *21*, 1038-1051.
10. Li, H.; Santos, F.; Butler, K.; Herndon, E., A critical review on the multiple roles of manganese in stabilizing and destabilizing soil organic matter. *Environ. Sci. Technol.* **2021,** *55*, 12136-12152.
11. Van Der Kellen, I.; Derrien, D.; Ghanbaja, J.; Turpault, M.-P., Recent weathering promotes C storage inside large phyllosilicate particles in forest soil. *Geochim. Cosmochim. Acta* **2022,** *318*, 328-351.
12. Rennert, T.; Handel, M.; Hoschen, C.; Lugmeier, J.; Steffens, M.; Totsche, K. U., A NanoSIMS study on the distribution of soil organic matter, iron and manganese in a nodule from a Stagnosol *Eur. J. Soil Sci.* **2014,** *65*, 684-692.
13. Lützow, M. V.; Kögel-Knabner, I.; Ekschmitt, K.; Matzner, E.; Guggenberger, G.; Marschner, B.; Flessa, H., Stabilization of organic matter in temperate soils: Mechanisms and their relevance under different soil conditions—a review. *Eur. J. Soil Sci.* **2006,** *57*, 426-445.
14. Wang, Y.; Stone, A. T., Reaction of $Mn^{III,IV}$ (hydr)oxides with oxalic acid, glyoxylic acid, phosphonoformic acid, and structurally-related organic compounds. *Geochim. Cosmochim. Acta* **2006,** *70*, 4477-4490.
15. Gulley-Stahl, H.; Hogan II, P. A.; Schmidt, W. L.; Wall, S. J.; Buhrlage, A.; Bullen, H. A., Surface complexation of catechol to metal oxides: An ATR-FTIR, adsorption. and dissolution study. *Environ. Sci. Technol.* **2010,** *44*, 4116-4121.
16. Flynn, E. D.; Catalano, J. G., Reductive transformations of layered manganese oxides by small organic acids and the fate of trace metals. *Geochimica et Cosmochimica Acta* **2019,** *250*, 149-172.
17. Wang, Y.; Stone, A. T., The citric acid-$Mn^{III,IV}O_2$(birnessite) reaction. Electron transfer, complex formation, and autocatalytic feedback. *Geochim. Cosmochim. Acta* **2006,** *70*, 4463-4476.
18. Luther III, G. W.; de Chanvalon, A. T.; Oldham, V. E.; Estes, E. R.; Tebo, B. M.; Madison, A. S., Reduction of manganese oxides: Thermodynamic, kinetic and mechanistic considerations for one- versus two-electron transfer steps. *Aqua. Geochem.* **2018,** *24*, 257-277.
19. Trainer, E. L.; Ginder-Vogel, M.; Remucal, C. K., Selective reactivity and oxidation of dissolved organic matter by manganese oxides. *Environ. Sci. Technol.* **2021,** *55*, 12084-12094.
20. Wang, Q.; Yang, P.; Zhu, M., Structural transformation of birnessite by fulvic acid under anoxic conditions. *Environ. Sci. Technol.* **2018,** *52*, 1844-1853.

21. Noerpel, M. R.; Lenhart, J. J., The impact of particle size on the adsorption of citrate to hematite. *J. Colloid Interface Sci.* **2015,** *460*, 36-46.
22. Campbell, E. R.; Warsko, K.; Davidson, A. M.; Bill Campbell, W. H., Determination of phosphate in soil extracts in the field: A green chemistry enzymatic method. *MethodsX* **2015,** *2*, 211-8.
23. Ravel, B.; Newville, M., ATHENA, ARTEMIS, HEPHAESTUS: data analysis for X-ray absorption spectroscopy using IFEFFIT. *J Synchrotron Radiat* **2005,** *12*, (Pt 4), 537-41.
24. Manceau, A.; Marcus, M.; Grangeon, S., Determination of Mn valence states in mixed-valent manganates by XANES spectroscopy. *Am. Mineral.* **2012,** *97*, 816-827.
25. McBride, M. B., Oxidation of 1,2- and 1,4-dihydroxybenzene by birnessite in acidic aqueous suspension. *Clays Clay Mineral.* **1989,** *37*, 479-486.
26. Chorover, J.; Amistadi, M. K., Reaction of forest floor organic matter at goethite, birnessite and smectite surfaces. *Geochim. Cosmochim. Acta* **2001,** *65*, 95-109.
27. Stone, A. T.; Morgan, J. J., Reduction and dissolution of manganese (III) and manganese (IV) oxides by organics. 1. Reaction with hydroquinone. *Environ. Sci. Technol.* **1984,** *18*, 450-456.
28. Majcher, E. H.; Chorover, J.; Bollag, J.; Huang, P. M., Evolution of CO_2 during birnessite-induced oxidation of ^{14}C-labeled catechol. *Soil Sci. Soc. Am. J.* **2000,** *64*, 157-163.
29. Loganathan, P. B., R. G., Sorption of heavy metal ions by a hydrous manganese oxide. *Geochim. Cosmochim. Acta* **1973,** *37*, 1277-1293.
30. Wang, Q.; Liao, X.; Xu, W.; Ren, Y.; Livi, K. J.; Zhu, M., Synthesis of Birnessite in the Presence of Phosphate, Silicate, or Sulfate. *Inorg. Chem.* **2016,** *55*, (20), 10248-10258.
31. Yin, H.; Li, H.; Wang, Y.; Ginder-Vogel, M.; Qiu, G.; Feng, X.; Zheng, L.; Liu, F., Effects of Co and Ni co-doping on the structure and reactivity of hexagonal birnessite. *Chem. Geol.* **2014,** *381*, 10-20.
32. Liu, M. M.; Cao, X. H.; Tan, W. F.; Feng, X. H.; Qiu, G. H.; Chen, X. H.; Liu, F., Structural controls on the catalytic polymerization of hydroquinone by birnessite. *Clays Clay Mineral.* **2012,** *59*, 525-537.
33. Stone, A. T.; Morgan, J. J., Reduction and dissolution of manganese (III) and manganese (IV) oxides by organics: 2. Survey of reactivity of organics. *Environ. Sci. Technol.* **1984,** *18*, 617-624.
34. Gao, M.; Zhang, Y.; Gong, X.; Song, Z.; Guo, Z., Removal mechanism of di-n-butyl phthalate and oxytetracycline from aqueous solutions by nano-manganese dioxide modified biochar. *Environ Sci Pollut Res Int* **2018,** *25*, (8), 7796-7807.
35. Khan, N. A.; Jung, B. K.; Hasan, Z.; Jhung, S. H., Adsorption and removal of phthalic acid and diethyl phthalate from water with zeolitic imidazolate and metal-organic frameworks. *J Hazard Mater* **2015,** *282*, 194-200.
36. Klewicki, J. K.; Morgan, J. J., Dissolution of β-MnOOH particles by ligands: Pyrophosphate, ethylenediaminetetraacetate, and citrate. *Geochim. Cosmochim. Acta* **1999,** *63*, 3017-3024.
37. Li, H.; Jaisi, D. P., An isotope labeling technique to investigate atom exchange during phosphate sorption and desorption. *Soil Sci. Soc. Am. J.* **2015,** *79*, 1340-1351.
38. Yu, J. S., P. E., Kinetics of MnO_2-catalyzed acetic acid oxidation in supercritical water. *Ind. Eng. Chem. Res.* **2000,** *39*, 4014-4019.
39. Shen, J.; Griffiths, P. T.; Campbell, S. J.; Utinger, B.; Kalberer, M.; Paulson, S. E., Ascorbate oxidation by iron, copper and reactive oxygen species: review, model development, and derivation of key rate constants. *Sci Rep* **2021,** *11*, (1), 7417.
40. Khamespanah, F.; Marx, M.; Crochet, D. B.; Pokharel, U. R.; Fronczek, F. R.; Maverick, A. W.; Beller, M., Oxalate production via oxidation of ascorbate rather than reduction of carbon dioxide. *Nat Commun* **2021,** *12*, (1), 1997.
41. Khan, Z.; Kumar, P.; Kabir ud, D., Kinetics of the reduction of water-soluble colloidal MnO2 by ascorbic acid. *Journal of Colloid and Interface Science* **2005,** *290*, (1), 184-189.
42. McBride, M. B., Oxidation of dihydroxybenzenes in aerated aqueous suspensions of birnessite. *Clays Clay Mineral.* **1989,** *37*, 341-347.
43. Colarieti, M. L.; Toscano, G.; Ardi, M. R.; Greco, G., Jr., Abiotic oxidation of catechol by soil metal oxides. *J Hazard Mater* **2006,** *134*, (1-3), 161-8.

44. Shindo, H.; Huang, P. M., Role of Mn(IV) oxide in abiotic formation of humic substances in the environment. *Nature* **1982,** *298*, 363-365.
45. McAlpine, R. D.; Cocivera, M.; Chen, H., Photooxidation and reduction of ascorbic acid studied by E.S.R. *Can. J. Chem.* **1973,** *51*, 1682-1686.
46. Maizel, A. C.; Remucal, C. K., Molecular Composition and Photochemical Reactivity of Size-Fractionated Dissolved Organic Matter. *Environ Sci Technol* **2017,** *51*, (4), 2113-2123.
47. Berg, S. M.; Whiting, Q. T.; Herrli, J. A.; Winkels, R.; Wammer, K. H.; Remucal, C. K., The Role of Dissolved Organic Matter Composition in Determining Photochemical Reactivity at the Molecular Level. *Environ Sci Technol* **2019,** *53*, (20), 11725-11734.
48. Feng, X. H.; Liu, F.; Tan, W. F.; Liu, X. W., Synthesis of birnessite from the oxidation of Mn^{2+} by O_2 in alkali medium: Effects of synthesis conditions. *Clays and Clay Minerals* **2004,** *52*, (2), 240-250.
49. Li, H.; Joshi, S. R.; Jaisi, D. P., Degradation and Isotope Source Tracking of Glyphosate and Aminomethylphosphonic Acid. *J Agric Food Chem* **2016,** *64*, (3), 529-38.
50. Stone, A. T., Reductive dissolution of manganese(III/IV) oxides by substituted phenols. *Environ. Sci. Technol.* **1987,** *21*, 979-988.
51. Lafferty, B. J.; Ginder-Vogel, M.; Zhu, M.; Livi, K. J. T.; Sparks, D. L., Arsenite oxidation by a poorly crystalline manganese-oxide. 2. Results from x-ray absorption spectroscopy and x-ray diffraction. *Environ. Sci. Technol.* **2010,** *44*, 8467-8472.
52. Zeng, C.; Yang, L.; Zhu, A. X.; Rossiter, D. G.; Liu, J.; Liu, J.; Qin, C.; Wang, D., Mapping soil organic matter concentration at different scales using a mixed geographically weighted regression method. *Geoderma* **2016,** *281*, 69-82.
53. Canarini, A.; Kaiser, C.; Merchant, A.; Richter, A.; Wanek, W., Root Exudation of Primary Metabolites: Mechanisms and Their Roles in Plant Responses to Environmental Stimuli. *Front Plant Sci* **2019,** *10*, 157.
54. Reisenauer, H. M., Determination of plant-available soil manganese. *In Manganese in soils and plants: Graham, R. D.; Hannam, R. J.; Uren, N. C. Eds.; Kluwer Academic Publishers, 1988; Chapter 6.* **1988**, 87-98.
55. Herndon, E. M.; Jin, L.; Andrews, D. M.; Eissenstat, D. M.; Brantley, S. L., Importance of vegetation for manganese cycling in temperate forested watersheds. *Global Biogeochemical Cycles* **2015,** *29*, (2), 160-174.
56. Jones, M. E.; LaCroix, R. E.; Zeigler, J.; Ying, S. C.; Nico, P. S.; Keiluweit, M., Enzymes, Manganese, or Iron? Drivers of Oxidative Organic Matter Decomposition in Soils. *Environ Sci Technol* **2020,** *54*, (21), 14114-14123.
57. Bourgault, R. R.; Rabenhorst, M. C., Manganiferous Soils in Maryland: Regional Extent and Field-Scale Electromagnetic Induction Survey. *Soil Science Society of America Journal* **2012,** *76*, (6), 2128-2135.

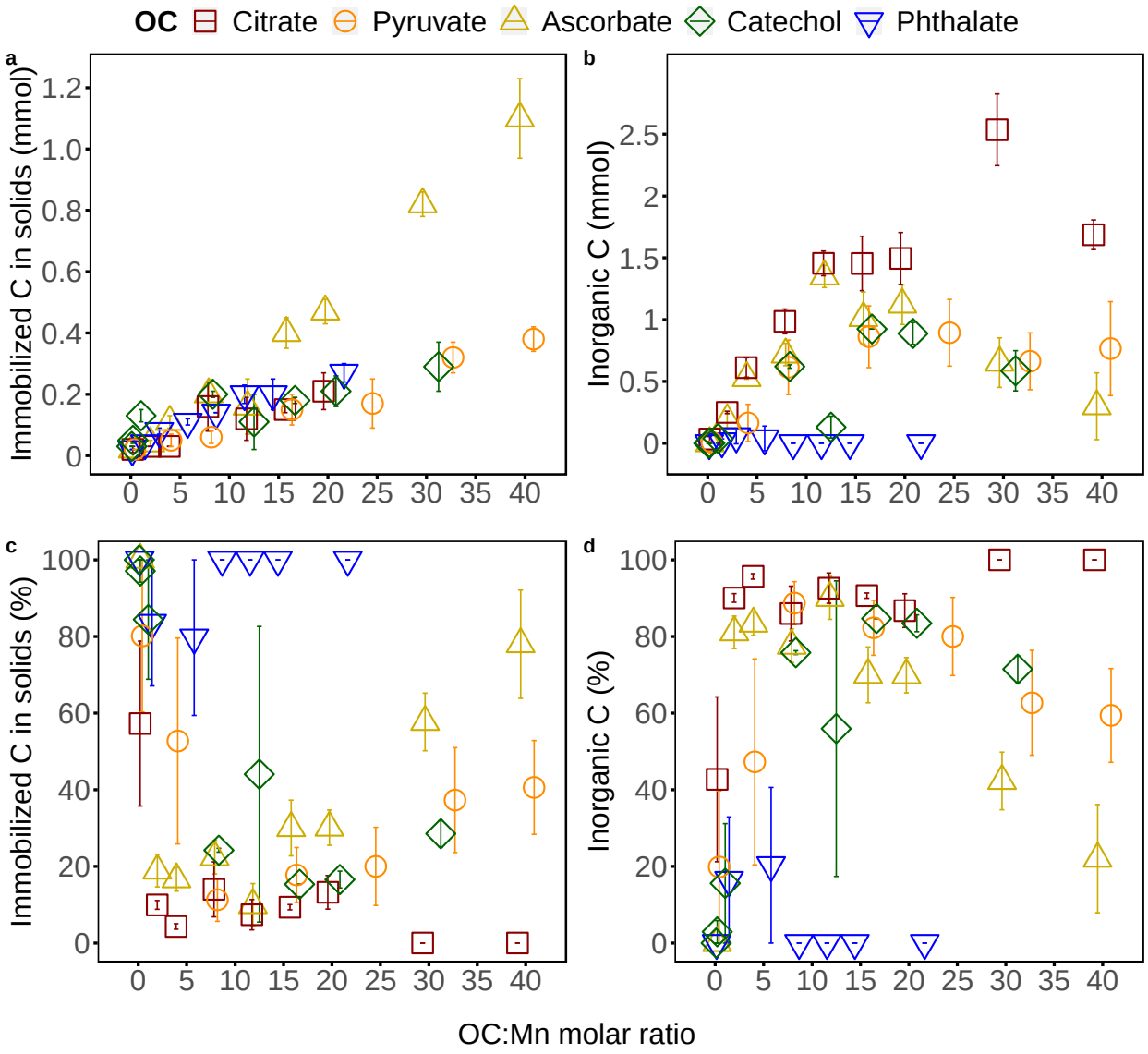

Figure 1. Amount of (a) immobilized C in solid phases and (b) inorganic C in solution and gaseous phases and the relative percentage of (c) immobilized C and (d) inorganic C to the total C loss as a function of initial OC to Mn molar ratios in the batch system. Error bars indicate standard errors among three Mn-oxides as triplicates.

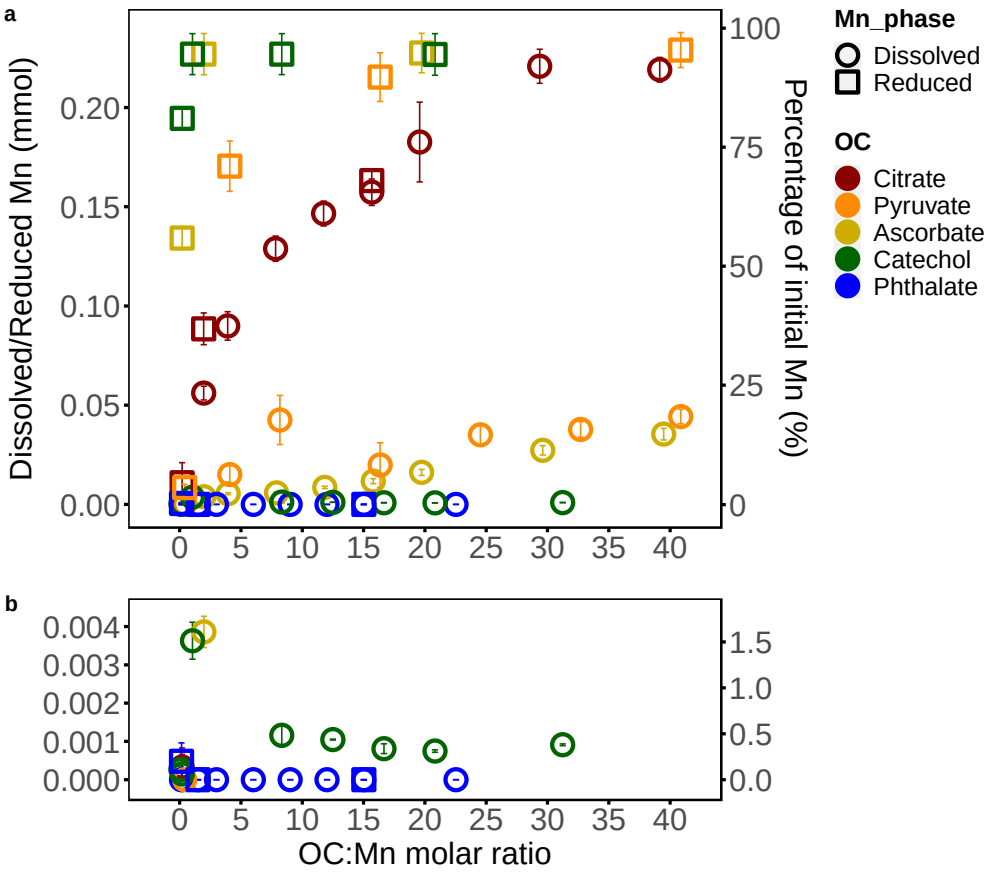

Figure 2. (a) The amount of dissolved (open circles) and total reduced Mn (open squares) and their corresponding percentage relative to the initial Mn in Mn-oxides, as a function of initial OC:Mn molar ratios in the batch system. The amount of total reduced Mn is the sum of dissolved Mn in aqueous phase and reduced Mn in solid phase as measured by XAS. Error bars indicate standard errors among three Mn-oxides as triplicates. (b) The zoomed-in view of the lower Mn amount region.

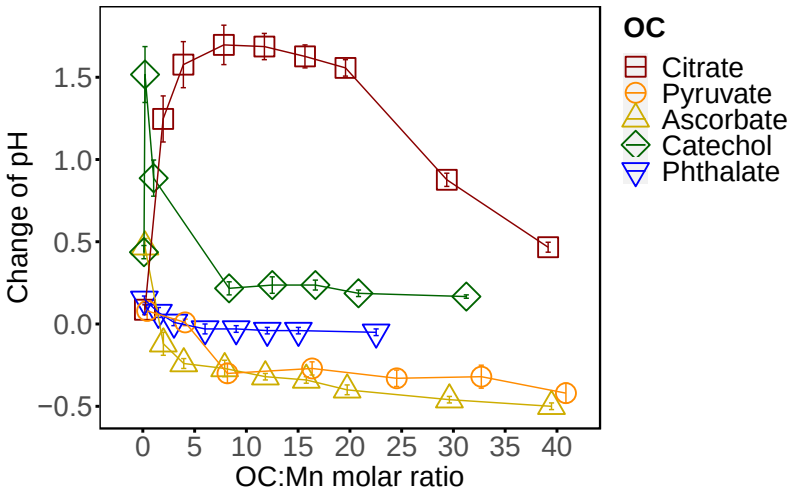

688

689 Figure 3. Change of equilibrium pH relative to control sets as a function of initial OC:Mn molar
690 ratios in the batch system.

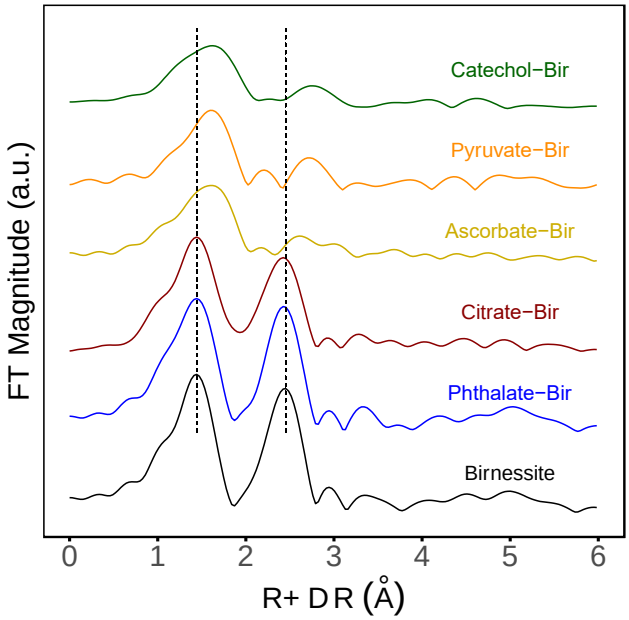

691

692 Figure 4. Magnitude of Fourier-transformed Mn K-edge EXAFS spectra of the Mn-oxides before
693 and after interactions with catechol, pyruvate, ascorbate, citrate, and phthalate at OC:Mn=21, 41,
694 20, 16, and 15, respectively.

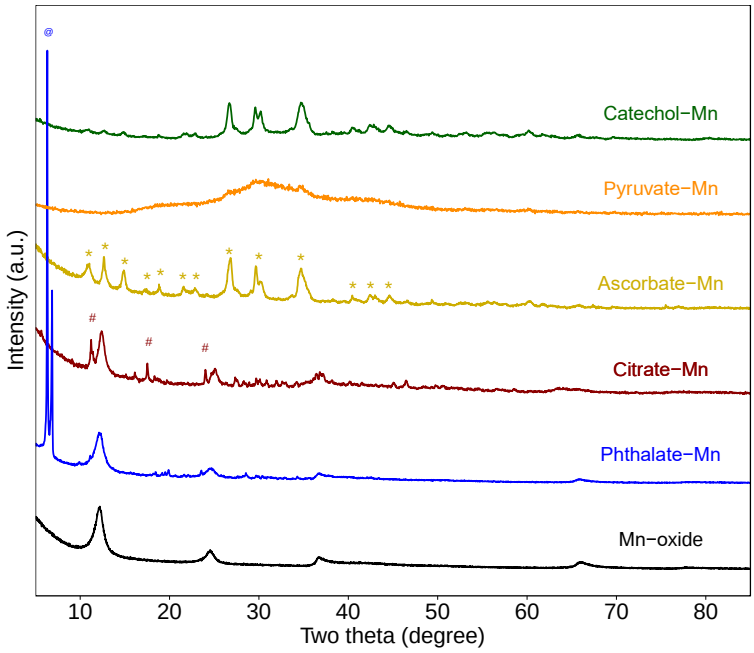

Figure 5. XRD patterns of the original Mn-oxide (birnessite in black) and catechol-, pyruvate-, ascorbate-, citrate-, and phthalate-associated minerals, at OC:Mn=21, 41, 20, 16, and 15, respectively. Yellow * indicates the characteristic peaks of manganese phosphate ($Mn_3(PO_4)_2$). Red # and blue @ represent for characteristic peaks of citrate and phthalate, respectively.

CONTACT INFORMATION

Hui Li

Department of Crop and Soil Sciences, North Carolina State University, Raleigh, NC 27695, United States

Environmental Sciences Division, Oak Ridge National Laboratory, Oak Ridge, TN 37831, United States

Benjamin Reinhart

X-ray Science Division, Argonne National Laboratory, Lemont, IL 60439, United States

Spencer Moller

Department of Plant and Soil Sciences, University of Delaware, Newark, DE 19716, United States

Elizabeth Herndon

Environmental Sciences Division, Oak Ridge National Laboratory, Oak Ridge, TN 37831, United States